IEEE Access
Multidisciplinary ⋮ Rapid Review ⋮ Open Access Journal

Received 17 January 2023, accepted 31 January 2023, date of publication 6 February 2023, date of current version 10 February 2023.

*Digital Object Identifier 10.1109/ACCESS.2023.3242979*

RESEARCH ARTICLE

# Optimizing Step-Size of Perturb & Observe and Incremental Conductance MPPT Techniques Using PSO for Grid-Tied PV System

**MOHAMMAD HAZIQ IBRAHIM[1], SWEE PENG ANG[1], MUHAMMAD NORFAUZI DANI[1], MOHAMMAD ISHLAH RAHMAN[2], (Member, IEEE), RAFIDAH PETRA[1], AND SHEIK MOHAMMED SULTHAN[1], (Senior Member, IEEE)**

[1]Electrical and Electronic Engineering Programme Area, Faculty of Engineering, Universiti Teknologi Brunei, Gadong BE1410, Brunei Darussalam
[2]School of Science and Engineering, Politeknik Brunei, Ministry of Education, Bandar Seri Begawan BA1311, Brunei Darussalam

Corresponding author: Mohammad Haziq Ibrahim (P20210003@student.utb.edu.bn)

**ABSTRACT** A maximum power point tracking (MPPT) technique plays an important role to ensure maximum photovoltaic (PV) output power is extracted under stochastic weather conditions. The research to date tends to focus on developing a standalone optimization MPPT algorithm rather than looking into a hybrid MPPT algorithm. This paper introduces particle swarm optimization (PSO) to optimize the maximum PV output power and to determine the best design variable for penalizing the step size of the conventional methods namely the perturb and observe (PO) and the incremental conductance (IC). With the help of the hybrid MPPT algorithm (PSO+IC and PSO+PO), the step size is no longer fixed, and it is changing according to the solar irradiance. To evaluate the proposed hybrid algorithm, a single-stage grid connected PV system is designed for several different scenarios with various weather conditions. The performance of the hybrid MPPT algorithm and the conventional methods is compared. The results demonstrate that the hybrid MPPT algorithm is remarkably better than the conventional methods, especially for PSO+IC, where it only takes 43.4 ms of tracking time and reaches the efficiency of 99.07% under standard test conditions.

**INDEX TERMS** Hybrid MPPT, particle swarm optimization, incremental conductance, perturb and observe, optimal step-size, single-stage grid connected PV system.

## I. INTRODUCTION

Due to the rising economic development and energy consumption, photovoltaic (PV) systems have been widely used in industry. One significant advantage of employing PV systems is that the sources are clean and less harmful to the environment compared to conventional power generation [1]. The ability of PV systems to reduce greenhouse gas emissions while producing power has made this system more reliable and robust. There are two widely used grid-tied inverters namely single-stage and double-stage inverters [2]. Single-stage grid connected PV systems comprise of dc/ac inverter with a transformer. Meanwhile, double-stage grid connected PV systems comprise of dc/ac inverter with a dc/dc boost converter. The power generation of the PV system highly depends on the weather conditions (i.e. solar irradiance and temperature), such that the output power will fluctuate due to the stochastic weather condition. Furthermore, the current against voltage and power against voltage curve shows a nonlinear relationship of the PV module. Thus, to harvest maximum power from the PV system, the maximum power point tracking (MPPT) algorithm is required and plays an important role in the PV system as discussed in [3].

Many researchers had proposed different types of algorithms and artificial intelligence techniques to determine the MPPT of the PV system. The most well-known algorithms used are the perturb and observe, and the incremental conductance. These methods are easy to implement and depend on the step change of the voltage or duty cycle [4]. Perturb and observe algorithm is based on the derivative of

The associate editor coordinating the review of this manuscript and approving it for publication was Lorenzo Ciani.

power in function of voltage is equal to zero at the maximum power point, meanwhile, the incremental conductance algorithm is based on comparing the values between PV array instantaneous current against voltage with the derivative of current in the function of voltage [5]. On the other hand, the artificial intelligence approach could be developed based on maximising the output power of the PV array.

In recent years, a modified MPPT algorithm was developed by many researchers with different applications which will be discussed as follows. In [6] and [7], an improved MPPT algorithm was developed based on the conventional incremental conductance and employed in a boost converter circuit. In [8] and [9], a modified incremental conductance was employed in a single-stage grid connected PV system. In [10], an improved perturb and observe algorithm was proposed and employed in the buck-boost converter circuit. In [11], a two-stage MPPT algorithm was proposed based on adaptive scaling factor beta, and perturb and observe algorithm was proposed and employed in the boost converter circuit. In [12], an improved variable step size of perturb and observe MPPT algorithm was developed and employed in the boost converter circuit. In [13], a modified perturb and observe MPPT was proposed and employed in a double-stage grid connected PV system. In [14], a high-performance variable step size perturb and observe MPPT algorithm was proposed and employed in a buck converter circuit. In [15], an improved MPPT control strategy was developed based on incremental conductance and was employed in the boost converter circuit. In [16], fast tracking incremental conductance algorithm was proposed and employed in the boost converter circuit. However, employing such an algorithm as discussed beforehand, highly depends on the step size voltage or duty cycle. Moreover, these techniques may not provide accurate tracking of the maximum power point (MPP) and it may result in an oscillation of voltage near the maximum power point. Therefore, to overcome these problems, optimization techniques had been widely developed by many researchers.

One major advantage of employing optimization techniques is the ability of the algorithm to determine the global optimum solution by generating random variables in the search space [17]. The capability of optimization techniques in many applications has made other researchers consider these methods to develop a better MPPT algorithm. In the past few years, many researchers have proposed an MPPT algorithm based on optimization techniques which will be discussed as follows. In [18], particle swarm optimization (PSO) has been employed to determine the MPPT by proposing two additional conditions namely the convergence detection and the change in solar insolation detection. In [19], an improved PSO-based MPPT was developed to reduce the steady state oscillation. In [20], the water cycle algorithm MPPT with the characteristics of power and current was proposed. In [21], a PSO-based global MPPT technique for distributed PV power generation with constraints for boost converters was proposed. In [22], a novel MPPT was proposed based on the Lagrange interpolation formula and PSO method. In [23], improved PSO, and perturb and observe MPPT algorithm were developed to reduce the oscillation during the MPPT phase. In [24], overall distribution and PSO MPPT algorithm were proposed to improve the tracking speed for maximum power point. In [25], a hybrid adaptive neuro-fuzzy inference system (ANFIS) and PSO-based MPPT method were proposed and employed in a zeta converter circuit to obtain rapid and zero oscillation tracking. In [26], an improved grey wolf optimizer MPPT algorithm was proposed and employed in boost full-bridge isolated converter (BFBIC) topology. In [27], an improved MPPT algorithm based on the earthquake optimization algorithm was proposed and employed in boost converter circuit to improve the dynamic behaviour of the PV systems. In [28], incremental conductance based on the PSO algorithm for MPPT was proposed and employed in the boost converter circuit. As discussed beforehand, most researchers tend to focus on developing a standalone optimization MPPT algorithm. The combination of optimization techniques and the conventional MPPT algorithms in standalone PV systems have shown improvement in the overall performance of the system [23], [28]. However, less effort is put into the work in integrating optimization techniques and the conventional methods for single-stage grid connected PV systems. It is expected to provide faster and more accurate tracking MPP which can improve the overall efficiency of the system. In addition, it can also make the system more robust and can adapt to different operating conditions.

In this paper, the method of improving the conventional methods namely the perturb and observe, and the incremental conductance by employing the optimization technique is presented. The method employed is to optimize the maximum PV output power and to determine the best design variable for penalizing the step size of the conventional methods. The results show that the combined methods lead to better efficiency and performance compared to the conventional methods.

The remainder of the paper is structured as follows. Section II describes the overview of the conventional MPPT algorithm. Section III describes the overview of the particle swarm optimization. Section IV describes the proposed MPPT algorithm based on particle swarm optimization. Section V provides the implementation and design of the single-stage grid connected PV system. Section VI discusses the results. Finally, Section VII concludes the paper.

## II. OVERVIEW OF THE CONVENTIONAL MPPT ALGORITHM

As discussed earlier, the most widely-known MPPT algorithms are the traditional perturb and observe, and incremental conductance. These algorithms are widely used due to their simplicity and effectiveness to track the MPP. Moreover, these algorithms are used as a baseline and they are considered standard references to make any comparisons

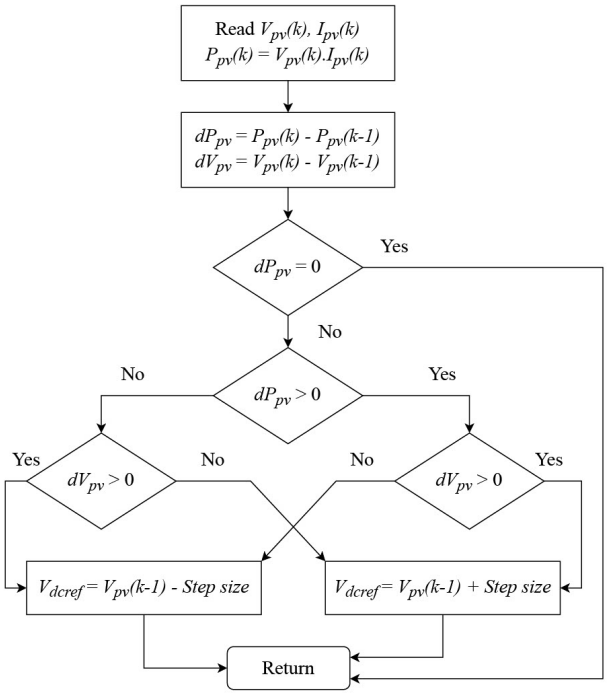


**FIGURE 1.** Flowchart of the conventional perturb and observe algorithm [14], [30], [33].

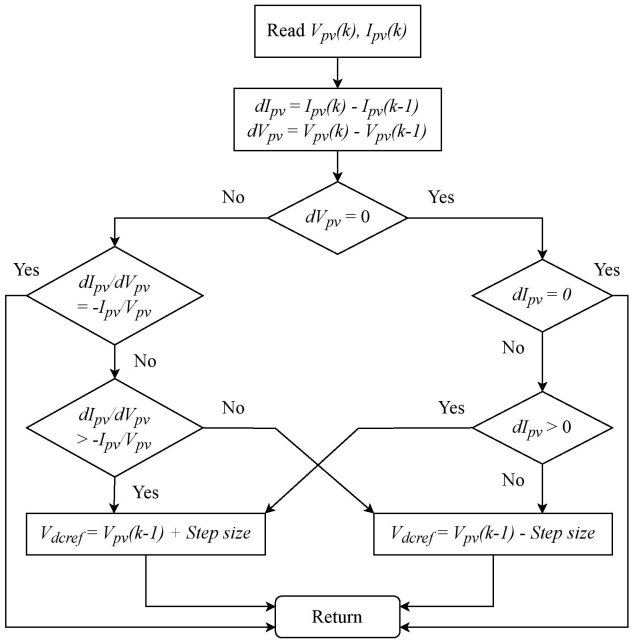


**FIGURE 2.** Flowchart of the conventional incremental conductance algorithm [31], [32], [33].

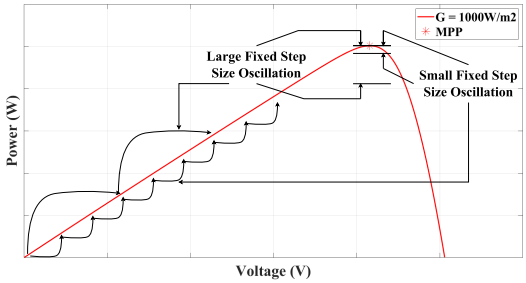


**FIGURE 3.** Comparison between small and large fixed step sizes oscillation at the MPP.

with new algorithms [14]. In this section, the overviews of both algorithms are discussed.

### A. PERTURB AND OBSERVE

Figure 1 shows the flowchart of the conventional perturb and observe algorithm. The voltage and current are measured from the PV module output to calculate the value of the output power. The difference in power and voltage is then calculated between the new values and the previous values. At the maximum operating point the change in power, $dP_{pv}$, is equal to zero. However, if $dP_{pv}$ is not equal to zero, the algorithm will try to find the best solution by increasing or decreasing the voltage with a fixed step size. If the operating point of the PV is on the left-hand side, the algorithm will track the MPP by driving the system to the right-hand side near the MPP and vice-versa.

### B. INCREMENTAL CONDUCTANCE

Figure 2 shows the flowchart of the incremental conductance algorithm. The voltage and current are measured from the PV module output. The value of change in voltage and current are calculated to determine the derivative of current in voltage. Moreover, the principle of the conventional incremental conductance algorithm is based on comparing the value between the derivative of current in the function of voltage and the PV array instantaneous current against voltage. This algorithm simply tracks the MPP by increasing or decreasing the reference voltage based on the operating point of the system. At MPP, the following conditions must be met [31], [32], [33]:

$$\frac{dP}{dV} = 0 \tag{1}$$

$$\frac{dP}{dV} = \frac{d(V \cdot I)}{dV} = I\frac{dV}{dV} + V\frac{dI}{dV} \tag{2}$$

$$\frac{dI}{dV} = -\frac{I}{V} \tag{3}$$

where $dI/dV$ is the derivative of current in the function of voltage, and $I/V$ is the PV instantaneous current against voltage. Furthermore, if $dI/dV > 0$, the reference voltage is increase based on fixed step voltage. Meanwhile, if $dI/dV < 0$ the reference voltage is decrease based on the fixed step voltage.

Both algorithms rely heavily on the step size that the user provides. Figure 3 shows the oscillation comparison between small and large fixed step sizes on the power against voltage curve. Small steady state oscillations are accomplished with small step sizes, but at the expense of a poor MPPT time response and a decline in output power efficiency. Meanwhile, using large step sizes enhances the

MPPT time response. However, the steady state oscillations near the maximum power point are amplified. Hence, in this paper, optimization is employed to maximize the output of PV power by penalizing and varying the step size which will be discussed further in this paper.

## III. OVERVIEW OF PARTICLE SWARM OPTIMIZATION

Particle swarm optimization algorithm can be simply described as fish schooling or a bird flocking searching for food in space, where it uses the velocity vector, the experience of each particle, and the experience of the neighbouring particle to generate a random position vector in the space [29]. The position of each particle in the space can calculated and updated based on the velocity equation given as [29]:

$$v_i^{(k+1)} = \alpha v_i^{(k)} + c_1 r_1^{(k)}[Pbest_i^{(k)} - x_i^{(k)}] + c_2 r_2^{(k)}[Gbest_i^{(k)} - x_i^{(k)}] \quad (4)$$

where $\alpha$ is a constant parameter called inertia weight. $c_1$ and $c_2$ are the cognitive coefficient and social coefficient of the particles respectively. $r_1^{(k)}$ and $r_2^{(k)}$ are the random numbers generated between 0 and 1. The new particle position vector can be calculated and updated as follow [29]:

$$x_i^{(k+1)} = x_i^{(k)} + v_i^{(k+1)} \quad (5)$$

In the search space, the particle will try to modify the position vector according to the velocity vector which could be calculated by the velocity equation and the distance of the particle from $Pbest_i^{(k)}$ and $Gbest_i^{(k)}$.

## IV. PROPOSED MPPT ALGORITHM BASED ON PARTICLE SWARM OPTIMIZATION

Due to the non-linearity behaviour of the PV module, accurate and fast dynamic response of MPPT is required. The performance of the MPPT is formulated by using both PSO and the conventional algorithm, which are presented in the flowchart of Figure 4. Initially, the irradiance, the voltage, and the current are sensed. This is followed by the objective function of the PV output power, $P_{pv}$, which can be defined as:

$$f = \max(P_{pv}) \quad (6)$$

$$P_{pv} = I_{pv} \times V_{pv} \quad (7)$$

where $I_{pv}$ is the output current of the PV module and $V_{pv}$ is the voltage of the PV module. In PSO, $I_{pv}$ and $V_{pv}$ are randomly initialized. The decision variables, $var$, can be expressed as:

$$var = [V_{pv}, I_{pv}] \quad (8)$$

The output current of the PV module, $I_{pv}$, is calculated based on IEC-61853 single diode model which can be extended as [34], [35]:

$$I_{pv} = I_L - I_o\left(\exp\left(\frac{V_{pv} + I_{pv}R_s}{\alpha_n}\right) - 1\right) - \frac{V_{pv} + I_{pv}R_s}{R_{sh}} \quad (9)$$

where $I_L$ is the light-generated current, $I_o$ is the reverse saturation current, $R_s$ is the series resistance, $R_{sh}$ is the parallel resistance, and $\alpha_n$ is the non-ideality factor.

In this model, an auxiliary equation is used to translate the five parameter to ten parameter model. The light-generated current, $I_L$, can be mathematically expressed as [34]:

$$\alpha_{ref} = \frac{N_s n K T_c}{q} \quad (10)$$

$$\alpha_n = \alpha_{ref} \cdot \frac{T_c}{T_{ref}} \quad (11)$$

$$I_L = \frac{G}{G_{ref}}(I_{L,ref} + \alpha_n[T_c - T_{ref}]) \quad (12)$$

where $N_s$ is the number of cells in the module, $n$ is the ideality factor, $K$ is the Boltzmann constant, $q$ is the charge of an electron, $G$ is the irradiance, $G_{ref}$ is the irradiance at standard reference condition (SRC), $T_c$ is the temperature, and $T_{ref}$ is the temperature at SRC. In addition, the diode reverse saturation current, $I_o$, can be mathematically expressed as [34]:

$$E_g = E_{g,ref}(1 - 0.0002677[T_c - T_{ref}]) \quad (13)$$

$$I_o = I_{o,ref}\left[\frac{T_c}{T_{ref}}\right]^3 \exp\left(\frac{1}{k}\left[\frac{E_g}{T_{ref}} - \frac{E_g}{T_c}\right]\right) \quad (14)$$

where $E_g$ is the energy bandgap, $E_{g,ref}$ is the energy band gap at SRC, and $I_{o,ref}$ is the diode saturation current reference at SRC. Other than that, the parallel resistance of the single diode model, $R_{sh}$, depends on the irradiance which can be mathematically expressed as [34]:

$$R_{sh} = R_{sh,ref} \cdot \frac{G_{ref}}{G} \quad (15)$$

where $R_{sh,ref}$ is the reference parallel resistance at SRC. Moreover, four constraints are taken into consideration. The first constraint is based on current against voltage curve characteristics, where it can be mathematically expressed as:

$$\frac{dI}{dV} = -\frac{1}{R_{sh}} - \frac{qI_o \exp\left(\frac{q(V_{pv} + I_{pv}R_s)}{nKTN_s}\right)}{nKTN_s} \quad (16)$$

where at the MPP, the first derivative of current in the function of voltage which is written in (16), must be equal to the instantaneous PV current divided by the instantaneous PV voltage. The second constraint is based on power against voltage curve characteristics, where it can be mathematically expressed as:

$$\frac{dP}{dV} = I_L - V_{pv}\left(\frac{1}{R_{sh}} + \frac{qI_o \exp\left(\frac{q(V_{pv} + I_{pv}R_s)}{nKTN_s}\right)}{nKTN_s}\right) - \frac{V_{pv} + I_{pv}R_s}{R_{sh}} - I_o\left(\exp\left(\frac{q(V_{pv} + I_{pv}R_s)}{nKTN_s}\right) - 1\right) \quad (17)$$

where at the MPP, the first derivative of power in the function of voltage is equal to zero. Meanwhile, the third and fourth constraints are to limit the search space of PSO, which can be mathematically expressed as:

$$0 < V_{pv} < V_{pv,max} \quad (18)$$

$$0 < I_{pv} < I_{pv,max} \quad (19)$$

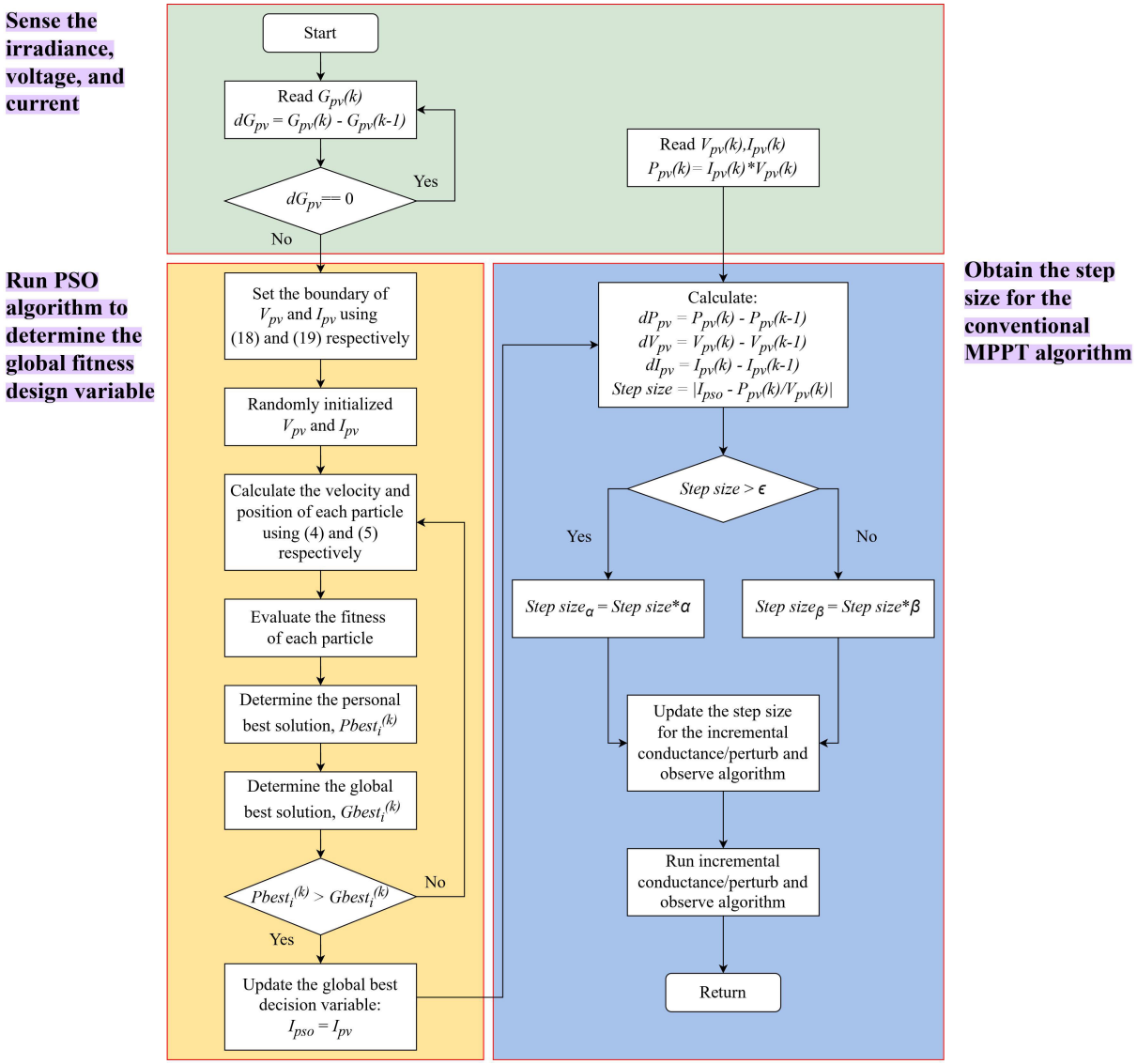


**FIGURE 4.** Flowchart of the proposed MPPT based on PSO.

where $V_{pv,max}$ and $I_{pv,max}$ are the open circuit voltage and the short circuit current of the PV module respectively.

At every iteration, PSO will update the best and the global best fitness value ever found in the search space. If the algorithm fails to determine the optimal solution, the decision variables are randomly re-initialized to search for the global best fitness value. The best design variable, $I_{pso}$, is then updated for the conventional MPPT algorithm to calculate the step size, which can be expressed as:

$$Step\ size = \left| I_{pso} - \frac{P_{pv}(k)}{V_{pv}(k)} \right| \tag{20}$$

Furthermore, a tolerance, $\epsilon$, is introduced to penalized the step size such that if the step size is greater than $\epsilon$, the new step size can be mathematically expressed as:

$$Step\ size_\alpha = Step\ size \times \alpha \tag{21}$$

where $\alpha$ is a large constant such that to enhance the performance of the MPPT by providing faster tracking time of the MPP during the change in weather conditions. Meanwhile, if the step size is less than $\epsilon$, the new step size can be mathematically expressed as:

$$Step\ size_\beta = Step\ size \times \beta \tag{22}$$

where $\beta$ is a small constant such that to enhance the performance of the MPPT by reducing the oscillation near the MPP during the steady-state condition. The calculated step size is then updated for the conventional MPPT algorithm.

## V. IMPLEMENTATION AND DESIGN OF SINGLE-STAGE GRID CONNECTED PV SYSTEM

Figure 5 shows the typical single-stage grid connected PV system control scheme. The system consists of a PV panel, dc-link voltage, dc/ac inverter, and LCL filter. The dc-link

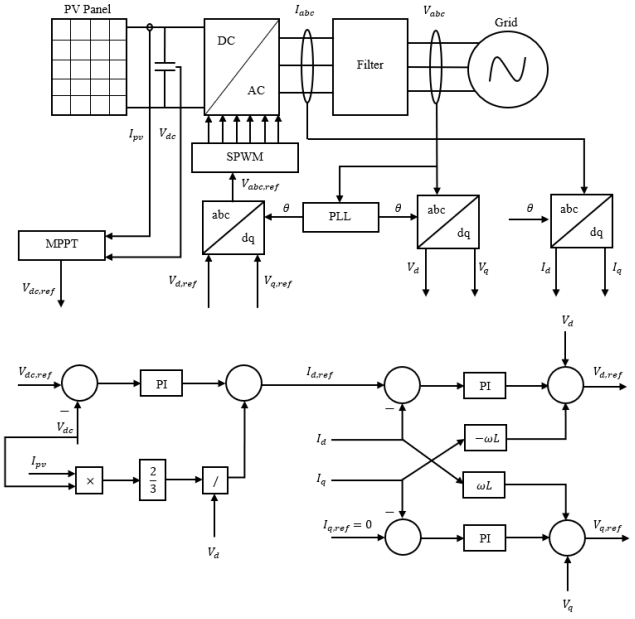


**FIGURE 5.** Single-stage grid connected PV system control scheme [8], [37], [38], [43].

voltage is regulated by using the outer loop voltage control (i.e., feed forward voltage regulator) to achieve low total harmonic distortion in the grid [39]. The outer loop utilises one PI controller to match the dc-link voltage with the reference voltage, $V_{dc,ref}$. Meanwhile, the inner loop current control utilises two PI controllers to regulate the direct current, $I_d$, and the quadrature current, $I_q$. The general relationship between the grid-tied inverter voltages and line currents can be expressed as [39]:

$$\begin{bmatrix} e_a \\ e_b \\ e_c \end{bmatrix} = R_f \begin{bmatrix} I_a \\ I_b \\ I_c \end{bmatrix} + L_f \frac{d}{dt} \begin{bmatrix} I_a \\ I_b \\ I_c \end{bmatrix} + \begin{bmatrix} V_a \\ V_b \\ V_c \end{bmatrix} \tag{23}$$

where $e_a$, $e_b$ and $e_c$ are the inverter output voltages, $I_a$, $I_b$ and $I_c$ are the three-phase line currents, $V_a$, $V_b$ and $V_c$ are the three-phase grid voltages, and $R_f$ and $L_f$ are the filter resistance and inductance respectively.

The synchronisation of the PV system to the grid is employed by converting three-phase electrical quantities to d-q axis quantities using Park's transformation, in which, a synchronous reference frame based phase-locked loop is employed [44]. The rotating reference frame synchronised with the grid voltage can be mathematically expressed as [39]:

$$V_d = e_d - R_f I_d + \omega L_f I_q - L\frac{dI_d}{dt} \tag{24}$$

$$V_q = e_q - R_f I_q - \omega L_f I_d - L\frac{dI_q}{dt} \tag{25}$$

where $V_d$ and $V_q$ are the grid d-axis and q-axis voltage components respectively, $e_d$ and $e_q$ are the d-axis and q-axis inverter voltage components respectively, $I_d$ and $I_q$ are the d-axis and q-axis grid currents respectively, and $\omega$ is the grid angular frequency.

**TABLE 1.** Grid-tied PV array simulation parameters [41], [42].

| Parameter | Value |
|---|---|
| Filter Inductance, $L_{filter,1}$,$L_{filter,2}$ | 500 $\mu$H |
| Filter Capacitance, $C_{filter}$ | 100 $\mu$F |
| DC-link Capacitance, $C_{dc-link}$ | 1000 $\mu$F |
| Grid Voltage, $V_{LL}$ | 415 V |
| Grid Frequency, $f$ | 50 Hz |
| Inverter Switching Frequency, $f_{sw}$ | 10 kHz |

**TABLE 2.** PV module specifications at 1000 W/m$^2$ and 25 °C [40].

| VBHN225SA06B Module Parameter | Value |
|---|---|
| Maximum Power, $P_{mpp}$ | 225.472 W |
| Cells per module, $N_{cell}$ | 72 |
| Open-circuit Voltage, $V_{oc}$ | 50.6 V |
| Short-circuit Current, $I_{sc}$ | 5.83 A |
| Voltage at MPP, $V_{mp}$ | 41.6 V |
| Current at MPP, $I_{mp}$ | 5.42 A |
| Temperature coefficient of $V_{oc}$ | -0.24%/ °C |
| Temperature coefficient of $I_{sc}$ | 0.0020069%/ °C |
| Light-generated current, $I_L$ | 5.8457 A |
| Diode saturation current, $I_D$ | $1.15\times10^{-12}$ A |
| Diode ideality factor, $n$ | 0.93611 |
| Shunt resistance, $R_{sh}$ | 242.2585 Ω |
| Series resistance, $R_s$ | 0.65124 Ω |
| Parallel strings, $N_{parallel}$ | 1 |
| Series-connected strings, $N_{series}$ | 1 |

**TABLE 3.** PV array specifications at 1000 W/m$^2$ and 25 °C [40].

| PV Array Parameter | Value |
|---|---|
| Maximum Power, $P_{mpp}$ | 1.003 MW |
| Open-circuit Voltage, $V_{oc}$ | 2530 V |
| Short-circuit Current, $I_{sc}$ | 518.87 A |
| Voltage at MPP, $V_{mp}$ | 2080 V |
| Current at MPP, $I_{mp}$ | 482.38 A |

In addition, in the synchronous rotating frame, the real power, $P_{grid}$, and the reactive power, $Q_{grid}$, can be expressed as [39]:

$$P_{grid} = \frac{3}{2}(V_d I_d + V_q I_q) \tag{26}$$

$$Q_{grid} = \frac{3}{2}(V_q I_d - V_d I_q) \tag{27}$$

The specification and relevant parameters of the grid-tied PV inverter are shown in Table 1. A Sanyo Electric Co Ltd of Panasonic Group VBHN-225S-A06B PV module is used and its output characteristics at standard test conditions are listed in Table 2. The PV array employed in this paper consists of 89 parallel strings and 50 series-connected strings of the VBHN-225S-A06B module. Table 3 shows the specification of the PV array at standard test conditions.

## VI. SIMULATION RESULTS AND ANALYSIS

Single stage grid connected PV system is simulated using the MATLAB/Simulink software with different MPPT

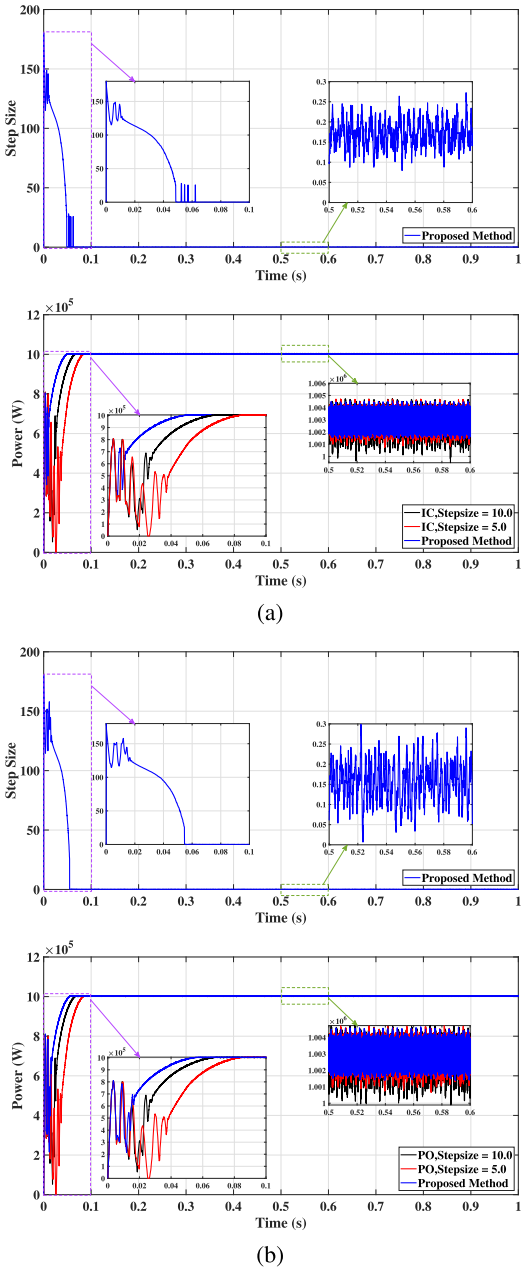


**FIGURE 6.** System response under standard test conditions; (a) Proposed method step size and PV output power comparison for incremental conductance, and (b) Proposed method step size and PV output power comparison for Perturb and Observe.

algorithms under varying input conditions, the obtained results are presented and discussed in this section. The performance of the proposed method (PSO+IC and PSO+PO) is compared with the conventional method (IC and PO). Four detailed simulation case studies were carried out under (i) Standard Test Conditions (1000 W/m$^2$, 25 $^o$C) (ii) Changing Irradiance Conditions, (iii) Changing Temperature Conditions, and (iv) Real Time Irradiance Conditions. In addition, the constant parameters of the PSO are listed in Table 4.

**TABLE 4.** Main parameters of the PSO algorithm.

| Parameter | Value |
|---|---|
| Inertia Weight, $\alpha$ | 1.0 |
| Cognitive Coefficient, $c_1$ | 1.5 |
| Social Coefficient, $c_2$ | 1.5 |

**TABLE 5.** Standard test conditions performance comparison between the proposed methods and the conventional methods.

| MPPT Algorithm | Step Size | Settling Time (ms) | $P_{Actual}$ (MW) | $\eta$ (%) |
|---|---|---|---|---|
| IC | 5 | 77.6 | 0.971 | 96.85 |
| | 10 | 60.5 | 0.983 | 97.98 |
| P&O | 5 | 77.6 | 0.971 | 96.85 |
| | 10 | 60.4 | 0.983 | 97.98 |
| Proposed IC | 0.01 to 180 | 43.4 | 0.994 | 99.07 |
| Proposed P&O | 0.01 to 180 | 49.5 | 0.990 | 98.73 |

### A. CASE 1: STANDARD TEST CONDITIONS

The output power with different MPPT algorithms and the step size of the proposed method are shown in Figure 6. It can be seen clearly that for a large fixed step size, the tracking of the MPP is much faster. However, there is a large oscillation of output power at a steady state. Meanwhile, for a small fixed step size, the tracking process is much slower. But, this will reduce the oscillation of output power at a steady state. Moreover, in comparison with the proposed methods, the step size generated varies from a larger step size (180) to a smaller step size (0.01). This improves the performance by providing faster tracking time and increases the efficiency of the output power as shown in Table 5. It must be noted that as the fixed step size of the conventional MPPT increases, the output power efficiency will decrease due to the increase in ripple output power, this affects the system performance in the long run. In addition, the efficiency of the output power, $\eta$, for each MPPT algorithm can be expressed as:

$$\eta = \frac{\int_0^t P_{Actual}}{\int_0^t P_{Theoretical}} \times 100\% \tag{28}$$

where $t$ is the time, $P_{Actual}$ is the actual output power generated from the PV system, and $P_{Theoretical}$ is the theoretical output power generated from the PV system. In Table 5, it must be noted that the $P_{Theoretical}$ is equal to 1.003 MW.

### B. CASE 2: CHANGING IRRADIANCE CONDITIONS

The changing irradiance is applied to the single stage grid connected PV system with constant temperature (25 $^o$C) as shown in Figure 7(a). The step size of the proposed method and the output power with different MPPT algorithms are shown in Figure 7(b) and 7(c) respectively. The output power of the system demonstrates that the step size provided by the proposed method is more precise in all situations.

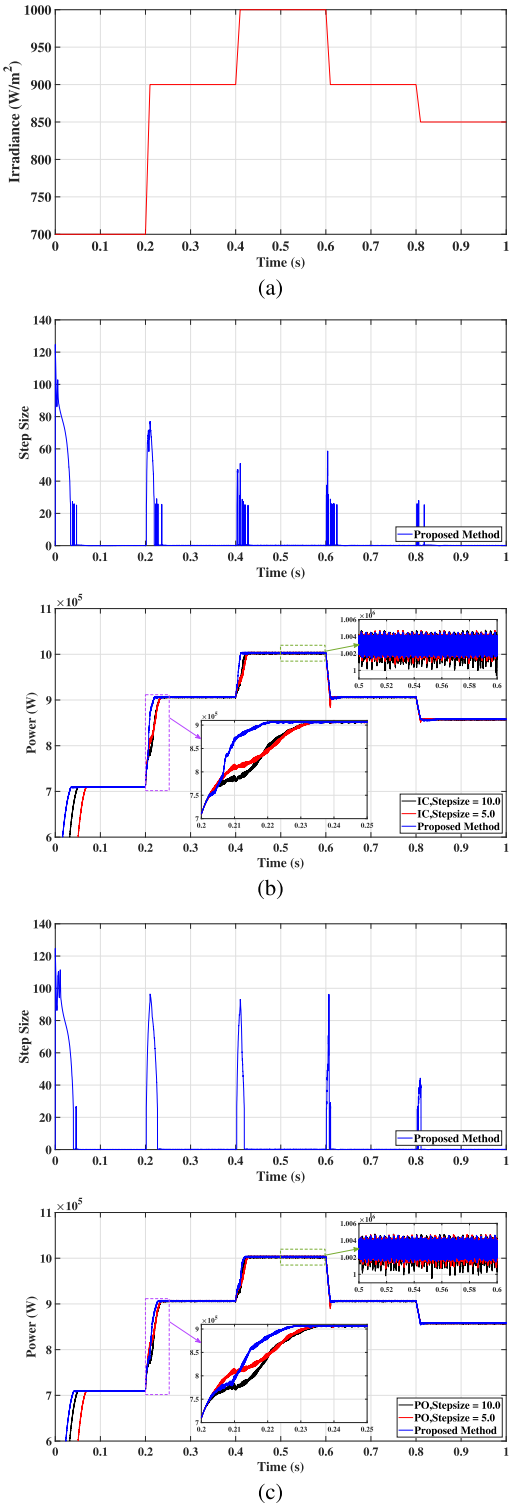


**FIGURE 7.** System response under changing irradiance conditions; (a) Changing irradiance profile, (b) Proposed method step size and PV output power comparison for incremental conductance, and (c) Proposed method step size and PV output power comparison for Perturb and Observe.

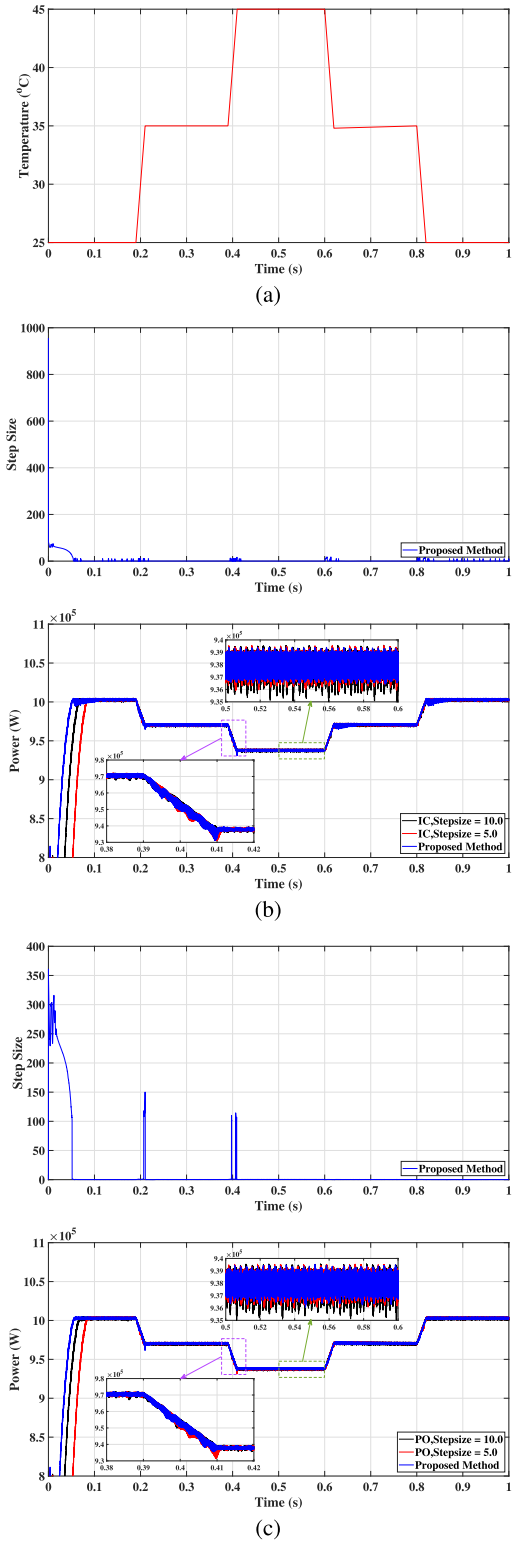


**FIGURE 8.** System response under changing temperature conditions; (a) Changing temperature profile, (b) Proposed method step size and PV output power comparison for incremental conductance, and (c) Proposed method step size and PV output power comparison for Perturb and Observe.

### C. CASE 3: CHANGING TEMPERATURE CONDITIONS

The changing temperature is applied to the same system with constant irradiance (1000 W/m$^2$) as shown in Figure 8(a). The step size of the proposed method and the output power with different MPPT algorithms are shown in Figure 8(b)

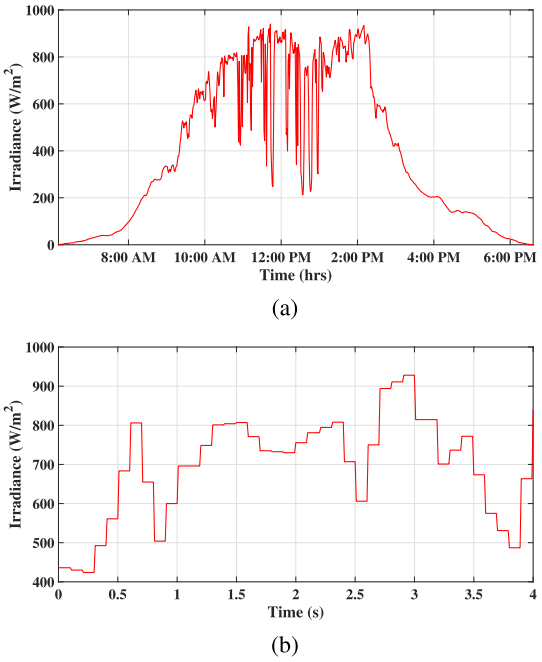


**FIGURE 9.** (a) Real time irradiance (b) Samples of irradiance.

and 8(c) respectively. The output power of the system demonstrates that the step size provided by the proposed method does not show any significant improvement to the system in terms of tracking time. Yet, the proposed algorithm is capable to reduce the ripple output power during the steady state condition.

### D. CASE 4: REAL TIME IRRADIANCE CONDITIONS

The performance of the proposed method under rapidly changing irradiance and constant temperature (25 $^{o}$C) is studied using real-time data samples. The real-time data was gathered from the weather station, where it collects the irradiance data at a sample rate of 60 s using the sensor and it is stored in the database in 60 s intervals. Figure 9(a) shows the rapid changes in the irradiance on a particular day in early June month in 2022. In order to simulate abruptly changing irradiance, 40 data samples of irradiance are collected at regular intervals from 10:55 AM to 11:15 AM. The collected data is given as a step input and it is considered that the changes are occurring every 0.1 s as shown in Figure 9(b).

The output power results of employing the conventional fixed small step size, large fixed step size, and the proposed method are shown in Figure 10. It can be seen clearly that, when there is a sudden change in irradiance, the proposed method offers a fast tracking time with lower ripple output power. Furthermore, the grid side results are tested with both the conventional and the proposed methods. It is assumed that the results are obtained as the system has been synchronised with the utility grid. Figure 11 and 12 show the d-q axis currents and the active and reactive power respectively. It can be seen clearly that the active power and active

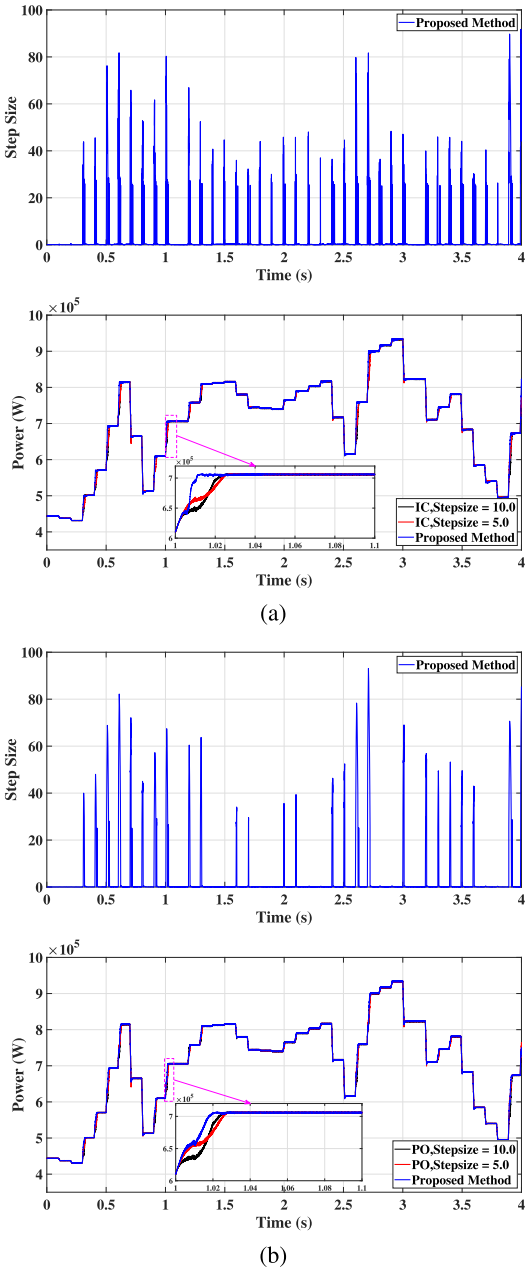


**FIGURE 10.** System response under real time irradiance conditions; (a) Proposed method step size and PV output power comparison for incremental conductance, and (b) Proposed method step size and PV output power comparison for perturb and observe.

current follow the irradiance shape under rapid changes. This is due to the output reference voltage, $V_{dc,ref}$, from the MPPT being fed into the outer loop voltage control. Whereas the reactive power and reactive current do not follow the irradiance shape due to the current controller q-axis, $I_{q,ref}$, being set equal to zero to ensure unity power factor operation. It is clear that by employing the proposed method, the grid side results and the PV side results are both improved in terms of their settling time and ripple output power.

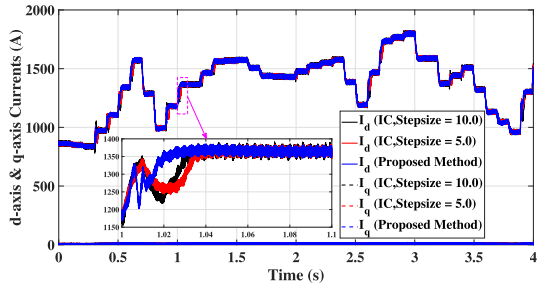


(a)

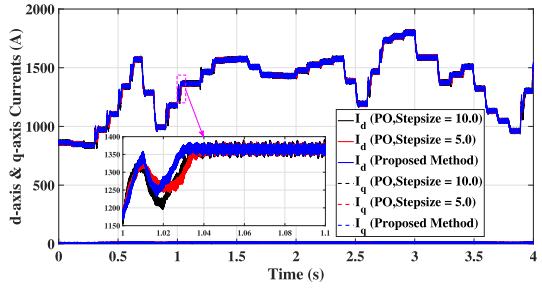


(b)

**FIGURE 11.** Grid side results: d-axis and q-axis currents comparison for (a) Incremental conductance, and (b) Perturb and observe.

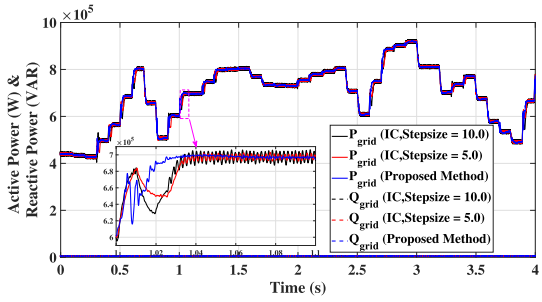


(a)

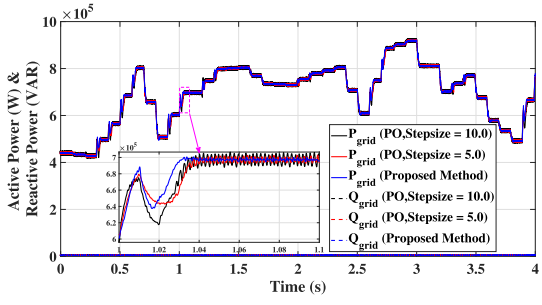


(b)

**FIGURE 12.** Grid side results: Active and reactive power comparison for (a) Incremental conductance, and (b) Perturb and observe.

## VII. CONCLUSION

In this paper, the proposed method (PSO+IC and PSO+PO) are employed for a single-stage grid-connected PV system. The proposed method is developed based on penalizing the step size by optimizing a single objective function problem with constraints, such that to maximize the output power of the PV system. The accuracy of the proposed method is verified and confirmed by comparing it with the conventional methods (IC and PO). A detailed case study is carried out under standard test conditions, changing irradiance conditions, changing temperature conditions, and real-time irradiance conditions. It was found that the proposed method improves the system efficiency by reducing the settling time (i.e. faster tracking time) and reduces the ripple output power (i.e. less oscillation at steady state). In future work, a detailed experimental case study which includes the proposed MPPT and the actual power system network with a large scale single-stage grid connected PV system will be implemented to further validate the results.

## REFERENCES

[1] F. Blaabjerg, R. Teodorescu, M. Liserre, and A. V. Timbus, "Overview of control and grid synchronization for distributed power generation systems," *IEEE Trans. Ind. Electron.*, vol. 53, no. 5, pp. 1398–1409, Oct. 2006, doi: 10.1109/TIE.2006.881997.

[2] Y. Huang, J. Wang, F. Z. Peng, and D.-W. Yoo, "Survey of the power conditioning system for PV power generation," in *Proc. 37th IEEE Power Electron. Spec. Conf.*, Jun. 2006, pp. 1–6.

[3] Y. Chaibi, A. Allouhi, M. Salhi, and A. El-Jouni, "Annual performance analysis of different maximum power point tracking techniques used in photovoltaic systems," *Protection Control Modern Power Syst.*, vol. 4, no. 1, pp. 1–10, Aug. 2019, doi: 10.1186/s41601-019-0129-1.

[4] W. Xiao and W. G. Dunford, "A modified adaptive Hill climbing MPPT method for photovoltaic power systems," in *Proc. IEEE 35th Annu. Power Electron. Spec. Conf.*, Jun. 2004, pp. 1957–1963.

[5] D. Sera, L. Mathe, T. Kerekes, S. V. Spataru, and R. Teodorescu, "On the perturb-and-observe and incremental conductance MPPT methods for PV systems," *IEEE J. Photovolt.*, vol. 3, no. 3, pp. 1070–1078, Jul. 2013.

[6] W. Ping, D. Hui, D. Changyu, and Q. Shengbiao, "An improved MPPT algorithm based on traditional incremental conductance method," in *Proc. 4th Int. Conf. Power Electron. Syst. Appl.*, Jun. 2011, pp. 1–4.

[7] S. Dhar, R. Sridhar, and G. Mathew, "Implementation of PV cell based standalone solar power system employing incremental conductance MPPT algorithm," in *Proc. Int. Conf. Circuits, Power Comput. Technol. (ICCPCT)*, Mar. 2013, pp. 1957–1963.

[8] V. N. Lal, M. Siddhardha, and S. N. Singh, "Control of a large scale single-stage grid-connected PV system utilizing MPPT and reactive power capability," in *Proc. IEEE Power Energy Soc. Gen. Meeting*, Jul. 2013, pp. 1–5.

[9] S. Ozdemir, N. Altin, and I. Sefa, "Single stage three level grid interactive MPPT inverter for PV systems," *Energy Convers. Manage.*, vol. 80, pp. 561–572, Apr. 2014.

[10] J. Ahmed and Z. Salam, "An improved perturb and observe (P&O) maximum power point tracking (MPPT) algorithm for higher efficiency," *Appl. Energy*, vol. 150, pp. 97–108, Jul. 2015.

[11] X. Li, H. Wen, L. Jiang, W. Xiao, Y. Du, and C. Zhao, "An improved MPPT method for PV system with fast-converging speed and zero oscillation," *IEEE Trans. Ind. Appl.*, vol. 52, no. 6, pp. 5051–5064, Nov. 2016.

[12] X. Serrano-Guerrero, J. Gonzalez-Romero, X. Cardenas-Carangui, and G. Escriva-Escriva, "Improved variable step size P&O MPPT algorithm for PV systems," in *Proc. 51st Int. Universities Power Eng. Conf. (UPEC)*, Sep. 2016, pp. 1–6.

[13] A. I. M. Ali, M. A. Sayed, and E. E. M. Mohamed, "Modified efficient perturb and observe maximum power point tracking technique for grid-tied PV system," *Int. J. Electr. Power Energy Syst.*, vol. 99, pp. 192–202, Jul. 2018.

[14] K. Saidi, M. Maamoun, and M. Bounekhla, "A new high performance variable step size perturb-and-observe MPPT algorithm for photovoltaic system," *Int. J. Power Electron. Drive Syst. (IJPEDS)*, vol. 10, no. 3, p. 1662, Sep. 2019.

[15] L. Shang, H. Guo, and W. Zhu, "An improved MPPT control strategy based on incremental conductance algorithm," *Protection Control Modern Power Syst.*, vol. 5, no. 1, pp. 1–8, Dec. 2020.

[16] M. Hebchi, A. Kouzou, and A. Choucha, "Improved incremental conductance algorithm for MPPT in photovoltaic system," in *Proc. 18th Int. Multi-Conf. Syst., Signals Devices (SSD)*, Mar. 2021, pp. 1271–1278.

[17] M. Abdel-Basset, L. Abdel-Fatah, and A. K. Sangaiah, "Metaheuristic algorithms: A comprehensive review," in *Computational Intelligence for Multimedia Big Data on the Cloud With Engineering Applications*. Elsevier, 2018, ch. 10, pp.185–231.

[18] M. Miyatake, M. Veerachary, F. Toriumi, N. Fujii, and H. Ko, "Maximum power point tracking of multiple photovoltaic arrays: A PSO approach," *IEEE Trans. Aerosp. Electron. Syst.*, vol. 47, no. 1, pp. 367–380, Jan. 2011.

[19] K. Ishaque, Z. Salam, M. Amjad, and S. Mekhilef, "An improved particle swarm optimization (PSO)–based MPPT for PV with reduced steady-state oscillation," *IEEE Trans. Power Electron.*, vol. 27, no. 8, pp. 3627–3638, Aug. 2012.

[20] M. Sarvi, I. Soltani, and I. N. Avanaki, "A water cycle algorithm maximum power point tracker for photovoltaic energy conversion system under partial shading condition," *Appl. Math. Eng., Manage. Technol.*, vol. 2, pp. 103–116, Jan. 2014.

[21] H. Renaudineau, F. Donatantonio, J. Fontchastagner, G. Petrone, G. Spagnuolo, J.-P. Martin, and S. Pierfederici, "A PSO-based global MPPT technique for distributed PV power generation," *IEEE Trans. Ind. Electron.*, vol. 62, no. 2, pp. 1047–1058, Feb. 2015.

[22] R. B. A. Koad, A. F. Zobaa, and A. El-Shahat, "A novel MPPT algorithm based on particle swarm optimization for photovoltaic systems," *IEEE Trans. Sustain. Energy*, vol. 8, no. 2, pp. 468–476, Sep. 2017.

[23] Z. Yang, Q. Duan, J. Zhong, M. Mao, and Z. Xun, "Analysis of improved PSO and perturb & observe global MPPT algorithm for PV array under partial shading condition," in *Proc. 29th Chin. Control Decis. Conf. (CCDC)*, May 2017, pp. 549–553.

[24] H. Li, D. Yang, W. Su, J. Lü, and X. Yu, "An overall distribution particle swarm optimization MPPT algorithm for photovoltaic system under partial shading," *IEEE Trans. Ind. Electron.*, vol. 66, no. 1, pp. 265–275, Jan. 2019.

[25] N. Priyadarshi, S. Padmanaban, J. B. Holm-Nielsen, F. Blaabjerg, and M. S. Bhaskar, "An experimental estimation of hybrid ANFIS–PSO-based MPPT for PV grid integration under fluctuating sun irradiance," *IEEE Syst. J.*, vol. 14, no. 1, pp. 1218–1229, Mar. 2020.

[26] K. Guo, L. Cui, M. Mao, L. Zhou, and Q. Zhang, "An improved gray wolf optimizer MPPT algorithm for PV system with BFBIC converter under partial shading," *IEEE Access*, vol. 8, pp. 103476–103490, 2020.

[27] E. Mendez, A. Ortiz, P. Ponce, I. Macias, D. Balderas, and A. Molina, "Improved MPPT algorithm for photovoltaic systems based on the earthquake optimization algorithm," *Energies*, vol. 13, no. 12, p. 3047, Jun. 2020.

[28] G. S. Chawda, O. P. Mahela, N. Gupta, M. Khosravy, and T. Senjyu, "Incremental conductance based particle swarm optimization algorithm for global maximum power tracking of solar-PV under nonuniform operating conditions," *Appl. Sci.*, vol. 10, no. 13, p. 4575, Jul. 2020.

[29] X. Dingyü, "Introduction to intelligent optimization methods," in *Solving Optimization Problems With MATLAB*. Berlin, Germany: De Gruyter, 2020, pp. 297–299.

[30] S. Bhattacharyya, P. D. S. Kumar, S. Samanta, and S. Mishra, "Steady output and fast tracking MPPT (SOFT-MPPT) for P&O and InC algorithms," *IEEE Trans. Sustain. Energy*, vol. 12, no. 1, pp. 293–302, Jan. 2021.

[31] S. Jain and V. Agarwal, "Comparison of the performance of maximum power point tracking schemes applied to single-stage grid-connected photovoltaic systems," *IET Electr. Power Appl.*, vol. 1, no. 5, p. 753, 2007.

[32] M. A. Elgendy, B. Zahawi, and D. J. Atkinson, "Assessment of the incremental conductance maximum power point tracking algorithm," *IEEE Trans. Sustain. Energy*, vol. 4, no. 1, pp. 108–117, Jan. 2013.

[33] R. I. Putri, S. Wibowo, and M. Rifa'i, "Maximum power point tracking for photovoltaic using incremental conductance method," *Energy Proc.*, vol. 68, pp. 22–30, Apr. 2015.

[34] A. P. Dobos and S. M. MacAlpine, "Procedure for applying IEC-61853 test data to a single diode model," in *Proc. IEEE 40th Photovoltaic Spec. Conf. (PVSC)*, Jun. 2014, pp. 2846–2849.

[35] P. Gilman, N. A. DiOrio, J. M. Freeman, S. Janzou, A. Dobos, and D. Ryberg, *SAM Photovoltaic Model Technical Reference Update*. Golden, CO, USA: National Renewable Energy Laboratory, 2018.

[36] K. T. Chaturvedi, M. Pandit, and L. Srivastava, "Self-organizing hierarchical particle swarm optimization for nonconvex economic dispatch," *IEEE Trans. Power Syst.*, vol. 23, no. 3, pp. 1079–1087, Aug. 2008.

[37] W. Libo, Z. Zhengming, and L. Jianzheng, "A single-stage three-phase grid-connected photovoltaic system with modified MPPT method and reactive power compensation," *IEEE Trans. Energy Convers.*, vol. 22, no. 4, pp. 881–886, Dec. 2007.

[38] F. Liu, S. Duan, P. Xu, G. Chen, and F. Liu, "Design and control of three-phase PV grid connected converter with LCL filter," in *Proc. IECON 33rd Annu. Conf. IEEE Ind. Electron. Soc.*, Nov. 2007, pp. 1656–1661.

[39] S. A. Lakshmanan, A. Jain, and B. S. Rajpourhit, "A novel current controlled technique with feed forward DC voltage regulator for grid connected solar PV system," in *Proc. 18th Nat. Power Syst. Conf. (NPSC)*, Dec. 2014, pp. 1–6.

[40] *MATLAB, Version R2022a*, MathWorks Inc., Natick, MA, USA, 2022.

[41] A. Reznik, M. G. Simões, A. Al-Durra, and S. M. Muyeen, "LCL filter design and performance analysis for grid-interconnected systems," *IEEE Trans. Ind. Appl.*, vol. 50, no. 2, pp. 1225–1232, Mar. 2014.

[42] M. A. Memon, "Sizing of DC-link capacitor for a grid connected solar photovoltaic inverter," *Indian J. Sci. Technol.*, vol. 13, no. 22, pp. 2272–2281, Jun. 2020.

[43] A. Yazdani and P. P. Dash, "A control methodology and characterization of dynamics for a photovoltaic (PV) system interfaced with a distribution network," *IEEE Trans. Power Del.*, vol. 24, no. 3, pp. 1538–1551, Jul. 2009.

[44] D. Haribabu, A. Vangari, and J. N. Sakamuri, "Dynamics of voltage source converter in a grid connected solar photovoltaic system," in *Proc. Int. Conf. Ind. Instrum. Control (ICIC)*, May 2015, pp. 360–365.

[45] S. S. Mohammed, D. Devaraj, and T. P. I. Ahamed, "A novel hybrid maximum power point tracking technique using perturb & observe algorithm and learning automata for solar PV system," *Energy*, vol. 112, pp. 1096–1106, Oct. 2016, doi: 10.1016/j.energy.2016.07.024.

**MOHAMMAD HAZIQ IBRAHIM** was born in Brunei Darussalam. He received the B.Eng. degree (Hons.) in electrical and electronic engineering from the University of Manchester, U.K., in 2020. He is currently pursuing the Ph.D. degree in electrical and elctronic engineering with Universiti Teknologi Brunei, Brunei Darussalam. His research interests include optimization, voltage stability, power systems, and solar PV systems.

**SWEE PENG ANG** was born in Brunei Darussalam. He received the B.Eng. degree (Hons.) in electronic and electrical engineering from the University of Glasgow, U.K., in 1995, the M.Sc. degree in electrical power engineering from the University of Manchester Institute Science and Technology (UMIST), U.K., in 2002, and the Ph.D. degree from the University of Manchester, U.K., in 2010. He is currently a Senior Assistant Professor with the Electrical and Electronic Engineering Programme Area, Universiti Teknologi Brunei, Negara, Brunei Darussalam. His research interests include transformer modeling, ferroresonance studies in power systems, solar power systems, and control in power systems.

**MUHAMMAD NORFAUZI DANI** received the B.Eng. degree (Hons.) in communication engineering from International Islamic University Malaysia (IIUM), the M.Sc. degree in radio frequency communication systems from the University of Southampton, U.K., and the Ph.D. degree in electrical and electronic engineering from the University of Manchester, U.K. From 2008 to 2015, he worked as a Manager in spectrum planning and numbering at the Authority for Info-Communications Technology Industry of Brunei Darussalam (AITI). He joined Universiti Teknologi Brunei (UTB), as a Lecturer, in 2015. His research interests include beyond 5G and 6G mobile networks, advanced multiple access schemes, wireless edge caching, broadcast/multicast networks, and optimization techniques.

**MOHAMMAD ISHLAH RAHMAN** (Member, IEEE) received the B.Eng. degree (Hons.) in electrical and electronic control engineering from the University of Aberdeen, U.K., and the M.E. degree in systems engineering from the University of Queensland, Australia, and the Ph.D. degree in electrical engineering from the University of Aberdeen, U.K. He is currently a Lecturer with Politeknik Brunei, Brunei. His research interests include renewable energy integration, DC/DC converters, HVDC, and control systems engineering.

**RAFIDAH PETRA** received the bachelor's degree in electrical and electronic engineering from Glasgow University, U.K., in 2004, under twinning programme with University Brunei Darussalam (UBD), and the master's degree in nanoelectronics and nanotechnology and the Ph.D. degree in electronics and electrical engineering from the University of Southampton, U.K. She is currently an Assistant Professor with the Faculty of Engineering, Universiti Teknologi Brunei (UTB), Brunei Darussalam. She has been working as an Educator, since she graduated the bachelor's degree (back in 2004), and progressively becomes an Active Academia, where she has been involved both in teaching and research. Her major is in silicon nano-photonics technology for telecommunications where she specializes on the design, fabrication, and characterization of nanoscale waveguide devices. Her expertise is in thin-film fabrication for devices at nanometer scale, for the application of solar cells and sensors for environmental sensing. Her current research interests include carbon dioxide (CO2) monitoring on the growth effect of vegetation through the use of technological engineering applications, investigation of direct air capture technology to alleviate the increase of atmospheric carbon dioxide (CO2) level, Brunei Darussalam, exploration of semiconductor nanostructured materials for solar energy harvesting and applications of nanotechnology for Halal authentication.

**SHEIK MOHAMMED SULTHAN** (Senior Member, IEEE) received the Ph.D. degree in electrical engineering. He has been working as an Assistant Professor with Universiti Teknologi Brunei, Brunei Darussalam. He has authored more than 50 papers in international journals and conference proceedings. He has published four patents and four book chapters. He is actively working on many funded projects mainly in the areas electric vehicles and solar PV systems. His research interests include solar PV systems, smart grid, microgrid, electric vehicles, low voltage DC systems, and machine learning.